Conformational dynamics of bacteriophage T7 DNA polymerase and its processivity factor, *Escherichia coli* thioredoxin

Barak Akabayov[1], Sabine R. Akabayov, Seung-Joo Lee, Stanley Tabor, Arkadiusz W. Kulczyk, and Charles C. Richardson[1]

Department of Biological Chemistry and Molecular Pharmacology, Harvard Medical School, Boston, MA 02115

Contributed by Charles C. Richardson, July 13, 2010 (sent for review May 11, 2010)

Gene 5 of bacteriophage T7 encodes a DNA polymerase (gp5) responsible for the replication of the phage DNA. Gp5 polymerizes nucleotides with low processivity, dissociating after the incorporation of 1 to 50 nucleotides. Thioredoxin (trx) of *Escherichia coli* binds tightly (Kd = 5 nM) to a unique segment in the thumb subdomain of gp5 and increases processivity. We have probed the molecular basis for the increase in processivity. A single-molecule experiment reveals differences in rates of enzymatic activity and processivity between gp5 and gp5/trx. Small angle X-ray scattering studies combined with nuclease footprinting reveal two conformations of gp5, one in the free state and one upon binding to trx. Comparative analysis of the DNA binding clefts of DNA polymerases and DNA binding proteins show that the binding surface contains more hydrophobic residues than other DNA binding proteins. The balanced composition between hydrophobic and charged residues of the binding site allows for efficient sliding of gp5/trx on the DNA. We propose a model for trx-induced conformational changes in gp5 that enhance the processivity by increasing the interaction of gp5 with DNA.

conformational transition | gene 5 protein | DNA replication | DNA-protein interactions

Bacteriophage T7 has evolved an efficient system for replicating its DNA (1). Four proteins account for most of the reactions that occur at the replication fork. Three of these proteins are encoded by the phage and one by the host. Therefore, phage T7 is able to bypass the more complicated *Escherichia coli* machinery. The four proteins are gene 5 DNA polymerase (gp5), *E. coli* thioredoxin (trx) processivity factor, gene 4 helicase-primase, and gene 2.5 ssDNA binding protein.

The crystal structure of gp5 in complex with trx, a primer template, and a nucleoside 5′-triphosphate in a polymerization mode is available (Fig. 1). The processivity factor, trx, binds tightly (5 nM) (2) in a one-to-one stoichiometry to a unique polypeptide loop (trx-binding domain) located in the thumb subdomain of gp5 (3) (Fig. 1). The binding of trx converts gp5 to a processive polymerase that polymerizes hundreds of nucleotides before dissociation from the DNA (4, 5). High processivity is an important property of replicative DNA polymerases that display high fidelity and a high rate of nucleotide polymerization (6). Two parameters that affect the processivity of DNA polymerases are often neglected: salt concentration and the sequence of the DNA template (6, 7).

How does trx increase the processivity of gp5? The crystal structure of gp5/trx bound to a primer template shows the trx-binding domain with the associated trx extended over the duplex region of the primer template (7). The trx-binding domain (TBD) and trx do not completely encircle the DNA as the other half of the DNA is resting in the DNA binding crevice of gp5. Nevertheless, the result is a clamp-like structure. The binding of trx most likely also orients the trx-binding domain so that additional basic residues contact the phosphodiester backbone of the DNA leading to a higher affinity for the DNA through increased electrostatic interactions (3). However, there is no structure of gp5 alone to serve as a reference to explain the structural effect of trx. Hence, other approaches are necessary to characterize the interaction of trx with gp5. Single-molecule studies suggest that thioredoxin increases the processivity by suppressing microscopic hopping on and off the DNA (8). Using neutron spin-echo spectroscopy, normal mode analysis, and a statistical-mechanical framework, Bu et al. (9) showed how protein domain motions are coupled during conformational changes within DNA polymerase I from *Thermus aquaticus*. Tang et al. (10) employed small-angle X-ray scattering (SAXS) and modeling studies as an alternative to crystallography to examine the conformational state of DNA polymerase β with a mismatched deoxyribonucleoside triphosphate (dNTP) in the active site. In these studies SAXS was used to monitor the conformational states of the enzyme to show that the ternary complex of DNA polymerase β-DNA-dNTP does not undergo conformational changes due to mis-incorporation of Mg-dNTP.

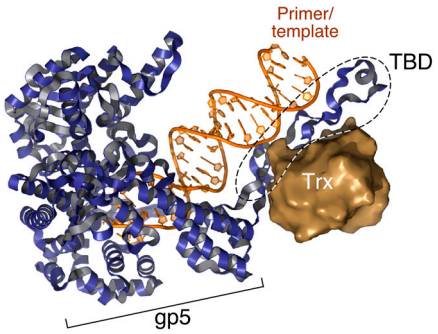

Fig. 1. Crystal structure of T7 gp5/trx bound to primer template and an incoming nucleotide. Gp5 is shown in blue and trx in brown. The DNA is shown in orange. Trx binds to the unique 76-residue segment at the tip of the thumb, trx-binding domain (TBD). [PDB ID code 1T8E (23)].

We have examined the conformational changes that occur in gp5 upon binding of trx. We present a model for an allosteric regulation of processivity by trx. Biochemical assays were used to study differences in DNA binding and dNTPs' incorporation between gp5 and gp5/trx. The processivity and rate of polymerization were determined using single-molecule techniques. We used SAXS and nuclease footprinting to examine conformational changes caused by trx binding to gp5. Our results show that conformational changes of gp5 that occur upon trx binding are responsible for the extension of the binding surface with DNA

Author contributions: B.A. and C.C.R. designed research; B.A., S.R.A., S.T., and A.W.K. performed research; S.-J.L. and S.T. contributed new reagents/analytic tools; B.A., S.R.A., A.W.K. and C.C.R. analyzed data; and B.A., S.R.A., and C.C.R. wrote the paper.

The authors declare no conflict of interest.

[1]To whom correspondence may be addressed. E-mail: ccr@hms.harvard.edu or barak_akabayov@hms.harvard.edu.

This article contains supporting information online at www.pnas.org/lookup/suppl/doi:10.1073/pnas.1010141107/-/DCSupplemental.

BIOCHEMISTRY

and ultimately for the increase in processivity. We have also compared the DNA interaction of the large fragment of *E. coli* Pol I (Klenow fragment) with those of the gp5/trx complex. The large fragment of the *E. coli* Pol I shares high sequence homology with gp5 with an identity of over 30% (11, 12) but does not bind trx.

Results

Influence of Ionic Strength on the Activity of Gp5. The processivity factor trx binds with high affinity (5 nM) to T7 gp5 in a 1:1 stoichiometry (2, 3) and converts it from an enzyme of low processivity to one of high processivity (5, 13). Trx increases the binding of gp5 to a primer-template 20–80-fold (5, 13). In these studies high salt concentration (100 mM NaCl) increased the efficiency of initiation of DNA synthesis but decreased processivity. The increased utilization of primers at high ionic strength was attributed to a reduction in nonspecific binding of gp5/trx to the DNA. The decrease in processivity was attributed to a change in the secondary structure of the DNA, perhaps arising from a neutralization of the repulsive charges on the DNA backbone. However, salt could also affect the charged residues of gp5/trx within the DNA binding crevice.

Gp5 alone is sensitive to increases in ionic strength as shown in Fig. 2*A*, where the activity on primed M13 DNA is reduced as the NaCl concentration is increased from 50 mM to 100 mM. At 125 mM NaCl where gp5 alone is inactive, gp5/trx retains 50% activity. The activity of gp5/trx is much greater than that of gp5 due to the increase in processivity, presumably resulting from the fewer rate limiting dissociation–association steps occurring during processive DNA synthesis.

We have also examined the effect of ionic strength on the binding of gp5 and gp5/trx to a primer template where the polymerase is trapped in a polymerization mode (Fig. 2*B*). In this analysis a primer template is incubated with T7 DNA polymerase in the presence of the next incoming dNTP. The 3′ terminus of the primer is occupied by a dideoxynucleotide and hence no nucleophilic attack can occur on the incoming dNTP. Such an approach was employed to obtain the crystal structure of gp5/trx in complex with a primer template and a dNTP (7). In the present experiments we have used a nitrocellulose filter binding assay to measure the amount of DNA bound to the polymerase at increasing concentrations of NaCl (Fig. 2*B*). Increasing the ionic strength leads to a significant difference in the binding of gp5 and gp5/trx to the DNA. Considerably higher salt concentrations are required to disrupt gp5/trx-DNA as compared to the gp5-DNA. At 110 mM NaCl gp5/trx is fully bound to the DNA, whereas only 50% of gp5 remains bound. Thus gp5 and gp5/trx bind to the primer template via two different modes as postulated recently (8).

The distribution of the electrostatic potentials on the structure of gp5/trx is presented in two different views of the complex in Fig. 2*C* where the negative values are in red and the positive in blue. Those residues in the DNA binding crevice that make contact with the DNA in the crystal structure are indicated by yellow dots. The DNA binding crevice has a highly positive potential, and the effect of salt may arise from a neutralization of this contact area with DNA. We propose that the differences in the behavior of gp5 and gp5/trx at high salt concentration arise from a different distribution of charged amino acids on the DNA binding interface. The binding of trx to gp5 leads to a conformational change that yields the electrostatic potential seen in Fig. 2*C*.

Leading-Strand Synthesis Observed at the Single-Molecule Level. The observation of interactions of a single protein with a DNA molecule in real time allows for the detection of intermediates and kinetic details that are difficult to obtain with ensemble assays. Single-molecule studies have shown that gp5, in the absence of trx, binds nonspecifically to duplex DNA and then diffuses along the DNA with frequent transient dissociations (8). However, upon binding trx the complex remains bound to the DNA while diffusing along the DNA. Single-molecule studies using optical tweezers have shown previously that the processivity of nucleotide polymerization of gp5/trx is 700 bases (14) as compared to only a few nucleotides by gp5 alone (6).

T7 gp5/trx cannot catalyze strand-displacement synthesis on duplex DNA (15). However, in the presence of gene 4 helicase leading-strand synthesis is observed (16). Gene 4 helicase unwinds double-stranded DNA and allows gp5/trx to extend the leading DNA strand. Both unwinding and polymerization activities are coordinated, and the proteins form an extremely stable complex (5). The processivity of leading-strand synthesis is greater than 17,000 nucleotides per binding event (17).

Trx is required for processive synthesis on ssDNA, but the question arises as to the role of trx in leading-strand synthesis. In the experiment shown in Fig. 3*A*, single-molecule techniques were used to measure the rate and processivity of leading-strand DNA synthesis catalyzed by gp5/trx and gp5 in a reaction with gene 4 helicase. The rates and processivities of leading-strand synthesis are presented in Fig. 3*B* along with examples of sin-

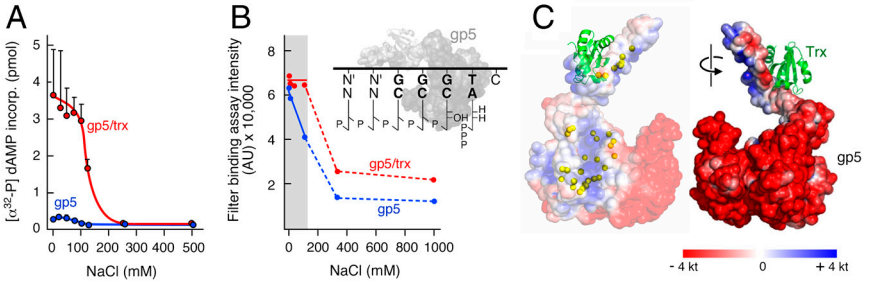

Fig. 2. Effect of ionic strength on polymerase activity and on the affinity of the polymerase for a primer template. Polymerase activity (*A*) was measured in the DNA polymerase assay containing 40 mM Tris-HCl, pH 7.5, 10 mM $MgCl_2$, 10 mM DTT, 50 mM potassium glutamate, 0.25 mM dTTP, dCTP, dGTP, and [α-^{32}P] dATP, 20 nM primed M13 DNA, and 5 nM gp5 in the absence of trx (blue) or in the presence of 25 nM trx (red), at the indicated concentrations of NaCl. After incubation at 37 °C for 10 min, the amount of [α-^{32}P] dAMP incorporated into DNA was measured. (*B*) The binding of gp5 and gp5/trx to a primer template in the presence of the incoming dNTP (see *Inset*) was measured using a nitrocellulose filter binding assay. The reaction contained 40 mM Tris-HCl, pH 7.5, 10 mM $MgCl_2$, 10 mM DTT, 50 mM potassium glutamate, 250 μM ddATP and ddGTP, and 2.5 μM gp5 in the presence (red) or absence (blue) of 3 μM trx and 1 nM primer template. The primer template consisted of the primer (5′-CGAAAACGACGGCCAGTGCCA-3′ annealed to the radiolabeled template strand 5′-^{32}P (5′-CCCCTTGGCACTGGCCGTCGTTTTCG-3′). The 3′-terminal nucleotide of the primer is ddCMP. The reaction mixture was loaded onto a nitrocellulose membrane laid atop a Zeta-probe membrane (see *Materials and Methods*) fixed on a dot microfiltration apparatus. The protein-DNA complex bound to the nitrocellulose membrane, and the free DNA on the Zeta-probe membrane were measured. (*C*) The distribution of electrostatic surface potentials for gp5/trx (7) calculated using the Adaptive Poisson-Boltzmann Solver plug-in (27) embedded in PyMol (www.pymol.org). The values of surface potentials are shown as a spectrum ranging from the negative value $-4kT$ (red) to the positive value $+4kT$ (blue). The residues in the DNA binding cleft that contact DNA are represented by yellow dots. Two different views of gp5/trx are presented.

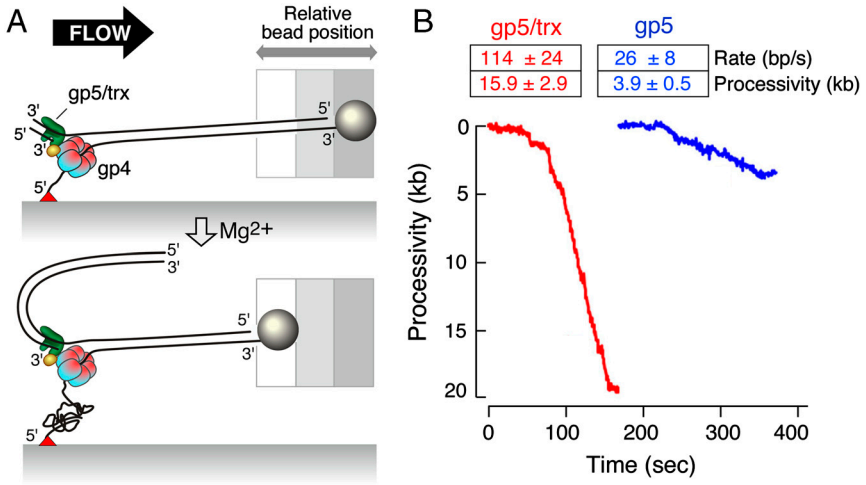

Fig. 3. Single-molecule analysis of leading-strand synthesis mediated by gp5/trx or gp5 in the presence of gp4 helicase. (*A*) Experimental design. Duplex λ DNA (48.5 kb) is attached to the surface of the flow cell via the 5′ end of the fork using biotin-streptavidin interaction, and the 3′ end is attached to a paramagnetic bead using digoxigenin-anti-digoxigenin interaction. The replication reaction in the flow cell contains 20 nM gp4 (hexameric concentration), 20 nM gp5/trx, or 100 nM gp5 in a buffer consisting of 600 μM each of dATP, dTTP, dCTP, and dGTP, 10 mM DTT, and 10 mM $MgCl_2$. DNA synthesis by proteins leads to conversion of the dsDNA to ssDNA, resulting in shortening of the DNA ligand that was accompanied by the movement of the bead against the direction of the flow. (*B*) Rate and processivity of leading-strand synthesis by gp5/trx or gp5 in the presence of gp4 helicase. Examples of single-molecule trajectories for leading-strand synthesis are shown. Rate and processivity were calculated by fitting the distributions of individual single-molecule trajectories using Gaussian and exponential decay distributions, respectively. Twenty-two single events were used to calculate rate and processivity for gp5/trx, and 11 events for gp5. Standard errors represent the accuracy in fitting of these distributions.

gle-molecule trajectories. Gp5/trx mediates strand-displacement synthesis with a processivity of 15.9 ± 2.9 kb and rate of 114± 24 nt/s, in good agreement with those previously reported (17). In contrast, the processivity of leading-strand synthesis for gp5 alone is 3.9 ± 0.5 kb, and the rate is 26 ± 8 nt/s. It is noteworthy that gp5 alone is able to interact with gp4 helicase to mediate leading-strand synthesis, albeit with a 4-fold decrease in both the rate and processivity.

Gp5 Adopts an Extended Global Conformation upon Binding of Trx. ***SAXS analysis.*** SAXS allows the characterization of structure and interactions of macromolecules in solution. The advent of high-flux synchrotron sources and advancement in data analysis enable the determination of low-resolution models from SAXS data. We used SAXS to study the conformational transition of gp5 upon binding of trx. The experimental SAXS pattern of gp5 (Fig. 4*A*) reflects structural characteristics in reciprocal space. The small-angle scattering curves and their corresponding Guinier plots are presented in Fig. S1. We have analyzed the small-angle region ($q = 0.0088$ to 0.38 Å^{-1}) of the scattering spectrum using the Guinier approximation and the software GNOM (18). Linearity of the small-angle part of the spectrum ($S^2 \leq 0.004$ Å^{-2}) in the Guinier plot indicates no aggregation of the sample that would hinder the analysis. An upward deviation from linearity in the wider-angle part of the spectrum (>0.004 Å^{-2}) of the gp5/trx complex corresponds to a more pronounced aberration from internal symmetry of the particles due to trx binding to gp5 (see Fig. S1). Such a deviation was shown previously for a myosin head subfragment-1 (19).

The analysis of the small-angle data of gp5/trx complex gives a hydrated radius of gyration (Rg) of 34 Å. This value is similar to the theoretical Rg calculated based on the crystal structure of gp5/trx [Protein Data Bank (PDB) ID code 1T8E] using CRYSOL (20) (Table 1) indicating that the crystal structure and the solution structure are comparable. The same analysis for the SAXS data of gp5 yielded an Rg of 31 Å (Table 1). To determine if this change in Rg was due to trx binding or to a conformational change, we calculated the theoretical scattering curve for gp5 by stripping the crystal structure of gp5 from DNA. The SAXS spectrum of free gp5 does not fit well with the theoretical scattering spectra of either free gp5 or gp5/trx derived from the crystal structure (PDB ID code 1T8E) with $\chi 2$ of 1.63 and 1.89, respectively. This deviation indicates that trx binding is accompanied by a conformation change between the free and bound gp5. The distance distribution function [$p(r)$] curve of free gp5 measures the distribution of pairwise distances (centers of mass) within the volume of the particle. The $p(r)$ of free gp5 shows a maximum dimension of the molecule (D_{max}) of 80 Å and

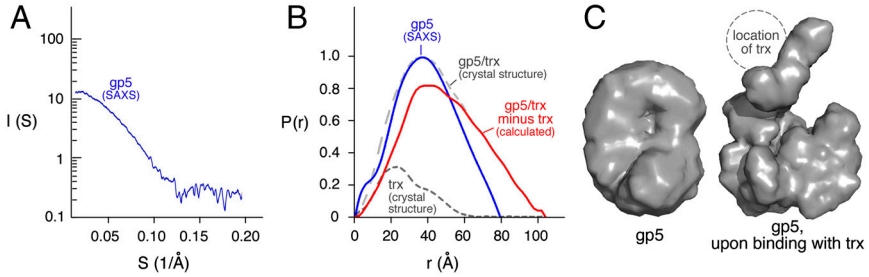

Fig. 4. SAXS data and low-resolution solution structure of gp5 and gp5/trx. (*A*) Low-angle data (0.0088–0.38 Å^{-1}) were obtained at a detector length of 2 m. (*B*) Distance distribution function $p(r)$ of free gp5 (blue) and gp5 upon binding to trx (red) with D_{max} of 80 Å and 105 Å, respectively. $p(r)$ was obtained using the computer program GNOM (18). The contribution of gp5 to the structure of gp5/trx was obtained by subtraction of the trx theoretical spectrum (PDB ID code 2trx, depicted in gray) from the gp5/trx theoretical spectrum (depicted in light dashed gray). (*C*) The corresponding ab initio model of gp5, obtained using the computer program GASBOR (20), is presented at *Left*. The gp5 contribution to the crystal structure of gp5/trx (PDB ID code 1T8E) is presented at *Right*.

Table 1. Overall parameters for X-ray scattering of gp5 and gp5/trx

Species	Method	R_g, Å	D_{max}, Å
Sphere*		27.87 (30.19)	
Gp5	Guinier†	31.5	
Gp5	Script‡	30.7	86
Gp5	GNOM§	30.8	80
Gp5/trx	CRYSOL¶	34	105
Gp5/trx	Guinier	33.3	
Gp5/trx	GNOM	34.9	104

R_g, radius of gyration; D_{max}, maximum dimension of particle.

*Calculated for spherical particle of 705 dummy beads corresponding to the number of amino acids in gp5 (and 827 corresponding to gp5/trx) when the diameter of individual bead is 2.1 Å.

†Determined by linear fitting to the Guinier region.

‡Our in-house script performs a course automatic search for the best fitting parameters using GNOM (Fig. S2) and is based on modifications of the search method described previously (25).

§Determined using the software GNOM (18). Results of the course search were refined to obtain a smooth $P(r)$.

¶Determined using the software CRYSOL (26) and the crystal structure of gp5/trx complex [PDB ID code 1T8E (23)].

has a maximum at 40 Å (Fig. 4*B*). The shape of the distribution with the maximum in the middle indicates a compact, sphere-like structure. Upon binding trx, the distribution becomes wider with a D_{max} of 105 Å (Table 1). This difference in D_{max} of 25 Å and the difference in shape with the maximum of the distribution shifting to the left cannot be explained by simple binding of trx, which is a relatively small molecule, but can be explained only by an elongation of the whole complex due to a conformational change. The theoretical $p(r)$ calculated from the crystal structure of gp5/trx (PDB ID code 1T8E) is consistent with the experimental $p(r)$ for the gp5/trx complex (Fig. S3). The software GASBOR (20) was used to reconstruct low-resolution structural models of free gp5. The average of 20 structural models (Fig. 4*C Left*) indicates that gp5 is more spherical relative to gp5/trx. The movement of the TBD relative to the polymerase core domain is the major conformational change upon trx binding as indicated by the shape of the molecular envelope obtained by SAXS.

Footprint of gp5 and gp5/trx on a primer template. We have examined the region of the primer template bound to gp5 and gp5/trx by determining the DNA protected from digestion by *E. coli* exonuclease III. Exonuclease III removes nucleotides sequentially from the 3′ ends of each strand of a DNA duplex (21). Either gp5 or gp5/trx was incubated with the primer template depicted in Fig. 5*A* where four nucleotides of the template strand are single-stranded. The primer bears a 3′ dideoxynucleotide and the next incoming nucleotide, in this case ddGTP, is present. These conditions lock the polymerase onto the primer template in a polymerization mode. The template strand is labeled with ^{32}P at its 5′ terminus. The resulting stable complex is then digested with exonuclease III, the DNA denatured, and the ^{32}P-labeled products identified by electrophoresis on a polyacrylamide gel (Fig. 5*B*).

When gp5 alone is bound to the primer template, 14 nucleotides of the template strand are protected from exonuclease III (Fig. 5*B*), precisely the number observed with the large fragment of *E. coli* Pol I (data not presented). However, when trx is present an additional 7 nucleotides are protected. Based on the orientation of the 3′-primer terminus and the 5′ terminus of the labeled template strand (Fig. 5*A*), gp5 protects 9 nucleotides (14 less the 5 nt present in the 5′-ssDNA tail of the template) of the duplex portion of the DNA adjacent to the primer terminus. The presence of trx extends this protection for an additional 7 nucleotides.

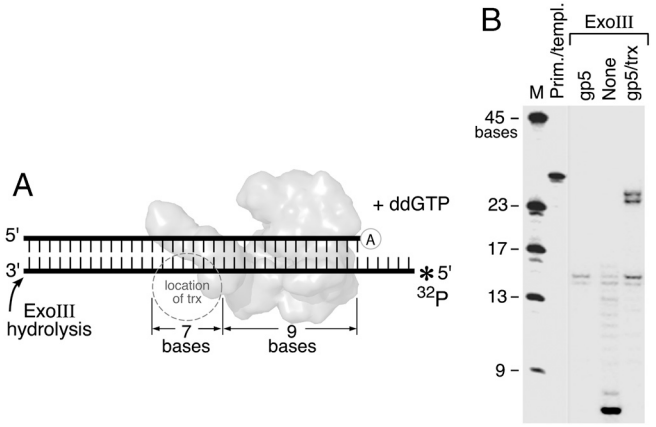

Fig. 5. Footprint of gp5 and gp5/trx on a primer template. (*A*) Schematic representation of gp5/trx bound to a primer template. The primer template used in this analysis consisted of a 5′-^{32}P radiolabeled 26-nt template annealed to a 21-nt primer strand such that there are five 5′-nucleotides of ssDNA on the template. ddATP and ddGTP are present in the reaction. Upon addition of DNA polymerase ddAMP is incorporated resulting in chain termination, and the next incoming nucleotide ddGTP cannot be incorporated but locks the polymerase onto the primer template. Gp5/trx has been superimposed on the DNA to create a model for the interpretation of the results. (*B*) Protection of the template strand from digestion by exonuclease III. The DNA primer template (500 pM) was incubated with 1 μM gp5 or gp5/trx. Reaction mixtures contained ddATP and ddGTP (250 μM). Exonuclease III (10 units) was added and the reaction was incubated at 37 °C for 10 min. The radiolabeled products were separated on 25% polyacrylamide gel containing 3 M urea and visualized by autoradiography.

The SAXS and exonuclease III footprinting studies complement each other and indicate that gp5 has a globular structure and, as a result, a smaller surface of interaction with DNA than does gp5 when bound to trx. The compact shape of the calculated structure based on SAXS data of gp5 fits the smaller DNA footprints.

Flexibility of the trx-binding loop. The flexibility of gp5 was characterized using normal mode analysis (NMA). NMA is a classical technique for studying the vibrational and thermal properties of molecular structures at the atomic level (22). NMA of gp5 based on the crystal structure of T7 DNA polymerase [gp5 only, PDB ID code 1T8E (23)] indicates that the trx-binding loop of gp5 possesses higher flexibility than the other regions of the protein (Fig. 6). The rmsd of the C-α atoms of the protein conformations as determined by NMA is related to the crystallographic B factor along the amino acid chain (Fig. 6).

Discussion

A number of processive proteins have been identified and their structures determined (24). Some enzymes, such as *E. coli* exonuclease I and the hexameric helicases achieve processivity by encircling the DNA. Others such as *E. coli* DNA polymerase III interact with an accessory protein that encircles the DNA. The mechanism of processivity for these proteins is relatively clear. There are, however, processive enzymes such as T7 RNA polymerase that only partially enclose their substrate. A major determinant for processivity with these proteins appears to be a large interactive surface (24).

How does T7 DNA polymerase achieve processivity? The polymerase itself has low processivity, and acquires high processivity only when it binds thioredoxin. The crystal structure of gp5 in complex with trx and a primer template (7) showed the DNA binding within the DNA binding crevice. A number of residues interact with the duplex portion of the DNA. In all of the polymerases of this family the thumb subdomain is located in a position above the DNA binding crevice that could at least partially enclose the DNA, perhaps contributing to their processivity.

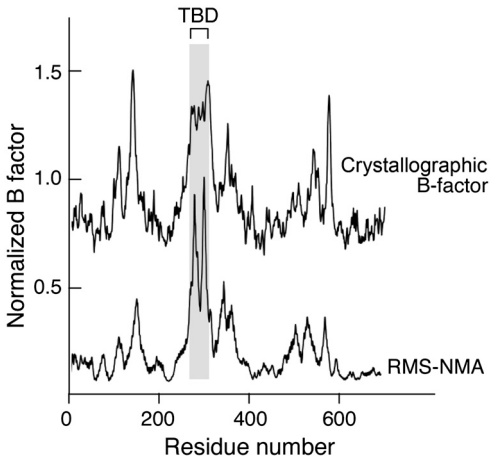

Fig. 6. Normal mode analysis (NMA) of gp5. NMA analysis (Web site: http://lorentz.immstr.pasteur.fr/gromacs/nma_submission.php) was carried out with the crystal structure of T7 DNA polymerase (PDB ID code 1T8E). The conformational changes of gp5 are depicted as obtained from NMA using 16 individual large domain-scale motions. The change in Cα conformation is presented.

In the T7 DNA polymerase trx binding to gp5 creates an extended sliding interface on the DNA.

In the crystal structure of T7 DNA polymerase trx is bound to a 76 amino acid polypeptide loop inserted between two helices in the thumb subdomain (7). Although trx is in a position to lock the DNA into the binding crevice, it is rotated away from the primer template. It is not unreasonable to speculate that trx and the flexible loop to which it is attached could swing across the DNA binding groove to encircle the DNA. Our finding that seven additional nucleotides of the primer template are protected from digestion by exonuclease III supports this model. We cannot rule out a trx-induced conformational change in gp5 that tightens the groove around the DNA or increases the interacting surface. A remaining question involves the mechanism by which the DNA moves within the groove during DNA synthesis. Upon the addition of each nucleotide, the DNA must slide to position the 3′ end of the primer into the active site for attack on the incoming nucleoside triphosphate. Trx and the trx-binding loop could secure the DNA by forming a lid over the DNA. In this model the mechanism is similar to that found in the β-protein clamp of *E. coli* DNA polymerase III. Alternatively, the trx-binding domain could make electrostatic interactions with the DNA and stabilize it. In either scenario each cycle of nucleotide addition necessitates a movement of the thumb to transiently release the DNA. Trx and the DNA binding crevice appear to be the major determinants of processivity as the trx-binding domain can be inserted into the comparable position in *E. coli* Pol I and trx then binds to this loop and confers processivity (3). Unfortunately, there is no structure of gp5 without trx bound to a primer template.

We have examined the effect of ionic strength on the formation of a stable complex with the primer template and gp5 or gp5/trx. Gp5 is more sensitive to salt than is gp5/trx, which is partially due to the increased DNA binding site of gp5/trx but may also reflect differences in the amino acids in the DNA binding cleft due to the conformational changes gp5 undergoes upon binding of trx. Ionic strength can affect the NTP binding site or the DNA binding site. In addition, changes in ionic strength can affect the charges on the phosphodiester backbone of the DNA or on the bases.

The DNA footprints obtained when either gp5 or gp5/trx is bound to DNA identify the DNA binding site and provide a measurement for the change in the gp5 surface of interaction with DNA upon binding of trx. The size of the binding site increases from 14 nt to 21 nt following the binding of trx. The additional nucleotides reside in the duplex portion of the primer template and more distal from the active site relative to those protected by gp5 alone. The footprints provide a low-resolution map of the protein's structure and a clue to the importance of trx to the DNA binding properties. We suggest that trx contributes to the interactions of gp5 with DNA in two ways. First, attachment: trx "sits" on the trx-binding domain and positions it such that it enhances the sliding interface of gp5. Second, trx induces conformational changes in gp5 that change the DNA binding cleft. Here we report the low-resolution solution structure of gp5 in the free state. We first obtained the radius of gyration and distance distribution function of gp5 and compared their values with those of gp5/trx. Then we modeled the structure of gp5 from the SAXS profile. The reconstructed structure was compared to the structure of gp5 from the crystal structure of T7 DNA polymerase. Our results demonstrate that gp5 has an end-to-end size (D_{max}) of 80 Å and R_g of 31 Å, whereas gp5/trx has a D_{max} of 105 Å and R_g of 34 Å. Any linear combination between the SAXS spectrum of gp5 and the theoretical spectrum of trx obtained from the crystal structure could not reproduce the spectrum of the complex species in solution. The inability to reproduce the complex spectrum is an indication that one of the components has changed its structure following binding to the other. Not only is gp5 12 times larger than trx, but there are also no differences between free trx and trx bound to gp5, comparing the available crystal structures. Therefore, the structural change occurs at the level of gp5. The contribution of gp5 to the spectrum of gp5/trx was obtained following subtraction of the weighted spectrum of trx from the spectrum of gp5/trx. Interpreting the experimental data using linear combination analysis yielded similar results that reproduced the spectrum of gp5 from the complex and trx components (Fig. S3). Overall, gp5 exhibits a markedly different conformation in the trx-bound state when compared to the free state. The shape of gp5 in the free state is more compact and symmetrical than is the shape of gp5 bound to trx. The size of both forms of gp5 is consistent with the measurements obtained from the DNA footprints.

Bu et al. showed how protein large motions are coupled during conformational changes within the Pol I from *Thermus aquaticus* (9). Another approach to determining the change in structure of gp5 resulting from the binding of trx is to compare the DNA binding surface of gp5/trx to that of the large fragment of *E. coli* Pol I (Fig. 7). The two are homologous enzymes with an amino acid sequence identity of 30%. Pol I, unlike gp5, does not bind to a processivity factor. Analysis of the amino acid composition of the DNA binding site of DNA binding proteins and DNA poly-

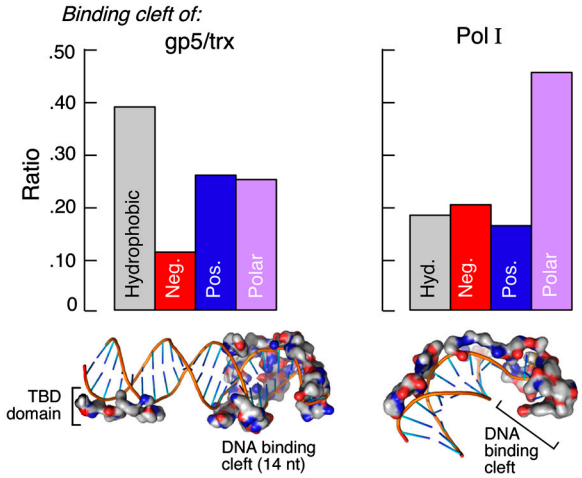

Fig. 7. Amino acids distribution in the DNA binding surface of T7 DNA polymerase and the large fragment of *E. coli* Pol I (Klenow fragment). The ratio between the type of amino acid (i.e., hydrophobic, negative, positive, or polar) and total number of amino acid residues constructing the DNA binding cleft of the enzymes is shown.

merases in general (Fig. S4) and of Pol I in comparison to gp5/trx specifically (Fig. 7) provides a structural basis for the difference in processivity. Using an in-house script, we analyzed the binding sites of all DNA binding proteins available in the Protein Data Bank and clustered them into two groups, all DNA binding proteins and DNA polymerases (Fig. S4). DNA polymerases have a larger percentage of hydrophobic residues and fewer positively charged residues within their binding surface than do DNA binding proteins in general.

The higher content of positively charged residues observed for all DNA binding proteins suggests a static binding mode dominated by electrostatic interactions (Fig. S4*B* and Table S1). The higher content of hydrophobic amino acids observed for polymerases reduces the specificity of binding and would allow the protein to slide more easily on the DNA. We suggest that the conformational change of gp5 due to trx binding results in a different composition of the DNA binding surface (Fig. 7). A comparison of the amino acid content of the DNA binding surface of gp5/trx to that of Pol I, presented in Fig. 7, shows that the ratio of hydrophobic/positive residues is higher in T7 DNA polymerase than in Pol I. We assume that the interaction surfaces of gp5 and Pol I are similar, but upon binding of trx gp5 changes its interaction surface with DNA.

In summary, a plausible model for the high processivity of the gp5/trx complex is that trx imposes a different conformation on the DNA binding groove (Fig. S5). The DNA binding surface increases and the corresponding amino acid composition of the interaction surface is altered. The consequence of the increased surface of interaction with DNA is a higher affinity for DNA and the ability to better slide on DNA.

Materials and Methods

Details of the assays can be found in *SI Text*. The activity of gp5 and gp5/trx was characterized by measuring the amount of radiolabeled dNTP incorporation. The interaction of gp5 and gp5/trx was examined by nuclease footprinting. The structure of gp5 was determined using SAXS and was compared to the crystal structure of gp5/trx. SAXS was measured at beamline X-9 at National Synchrotron Light Source, and the data were processed and analyzed using software applications embedded in the ATSAS package (http://www.embl-hamburg.de/ExternalInfo/Research/Sax/software.html).

ACKNOWLEDGMENTS. We thank Lin Yang (Beamline X-9 NSLS, BNL) for user support. We thank Antoine van-Oijen for providing the experimental setup used for the single molecule experiments. Use of the National Synchrotron Light Source, Brookhaven National Laboratory, was supported by the U.S. Department of Energy, Office of Science, Office of Basic Energy Sciences, under Contract DE-AC02-98CH10886.

1. Hamdan SM, Richardson CC (2009) Motors, switches, and contacts in the replisome. *Annu Rev Biochem* 78:205–243.
2. Huber HE, Russel M, Model P, Richardson CC (1986) Interaction of mutant thioredoxins of *Escherichia coli* with the gene 5 protein of phage T7: The redox capacity of thioredoxin is not required for stimulation of DNA polymerase activity. *J Biol Chem* 261:15006–15012.
3. Bedford E, Tabor S, Richardson CC (1997) The thioredoxin binding domain of bacteriophage T7 DNA polymerase confers processivity on *Escherichia coli* DNA polymerase I. *Proc Natl Acad Sci USA* 94:479–484.
4. Hamdan SM, et al. (2007) Dynamic DNA helicase-DNA polymerase interactions assure processive replication fork movement. *Mol Cell* 27:539–549.
5. Tabor S, Huber HE, Richardson CC (1987) *Escherichia coli* thioredoxin confers processivity on the DNA polymerase activity of the gene 5 protein of bacteriophage T7. *J Biol Chem* 262:16212–16223.
6. Von Hippel PH, Fairfield FR, Dolejsi MK (1994) On the processivity of polymerases. *Ann NY Acad Sci* 726:118–131.
7. Doublie S, Tabor S, Long AM, Richardson CC, Ellenberger T (1998) Crystal structure of a bacteriophage T7 DNA replication complex at 2.2 A resolution. *Nature* 391:251–258.
8. Etson CM, Hamdan SM, Richardson CC, van Oijen AM (2010) Thioredoxin suppresses microscopic hopping of T7 DNA polymerase on duplex DNA. *Proc Natl Acad Sci USA* 107:1900–1905.
9. Bu Z, Biehl R, Monkenbusch M, Richter D, Callaway DJ (2005) Coupled protein domain motion in Taq polymerase revealed by neutron spin-echo spectroscopy. *Proc Natl Acad Sci USA* 102:17646–17651.
10. Tang KH, et al. (2008) Mismatched dNTP incorporation by DNA polymerase beta does not proceed via globally different conformational pathways. *Nucleic Acids Res* 36:2948–2957.
11. Kornberg A, Baker TA (1992) *DNA Replication* (Freeman, San Francisco).
12. Ollis DL, Kline C, Steitz TA (1985) Domain of *E. coli* DNA polymerase I showing sequence homology to T7 DNA polymerase. *Nature* 313:818–819.
13. Huber HE, Tabor S, Richardson CC (1987) *Escherichia coli* thioredoxin stabilizes complexes of bacteriophage T7 DNA polymerase and primed templates. *J Biol Chem* 262:16224–16232.
14. Wuite GJ, Smith SB, Young M, Keller D, Bustamante C (2000) Single-molecule studies of the effect of template tension on T7 DNA polymerase activity. *Nature* 404:103–106.
15. Lechner RL, Richardson CC (1983) A preformed, topologically stable replication fork. Characterization of leading strand DNA synthesis catalyzed by T7 DNA polymerase and T7 gene 4 protein. *J Biol Chem* 258:11185–11196.
16. Notarnicola SM, Mulcahy HL, Lee J, Richardson CC (1997) The acidic carboxyl terminus of the bacteriophage T7 gene 4 helicase/primase interacts with T7 DNA polymerase. *J Biol Chem* 272:18425–18433.
17. Lee JB, et al. (2006) DNA primase acts as a molecular brake in DNA replication. *Nature* 439:621–624.
18. Svergun DI (1992) Determination of the regularization parameter in indirect-transform methods using perceptual criteria. *J Appl Crystallogr* 25:495–503.
19. Wakabayashi K, et al. (1992) Small-angle synchrotron x-ray scattering reveals distinct shape changes of the myosin head during hydrolysis of ATP. *Science* 258:443–447.
20. Svergun DI, Petoukhov MV, Koch MHJ (2001) Determination of domain structure of proteins from X-ray solution scattering. *Biophys J* 80:2946–2953.
21. Richardson CC, Lehman IR, Kornberg A (1964) A deoxyribonucleic acid phosphatase-exonuclease from *Escherichia coli*. II. Characterization of the exonuclease activity. *J Biol Chem* 239:251–258.
22. Tama F, Brooks CL (2006) Symmetry, form, and shape: Guiding principles for robustness in macromolecular machines. *Annu Rev Biophys Biomol Struct* 35:115–133.
23. Brieba LG, et al. (2004) Structural basis for the dual coding potential of 8-oxoguanosine by a high-fidelity DNA polymerase. *EMBO J* 23:3452–3461.
24. Breyer WA, Matthews BW (2001) A structural basis for processivity. *Protein Sci* 10:1699–1711.
25. Lipfert J, et al. (2007) Structural transitions and thermodynamics of a glycine-dependent riboswitch from Vibrio cholera. *J Mol Biol* 365:1393–1406.
26. Svergun DI, Barberato C, Koch MHJ (1995) CRYSOL—a program to evaluate X-ray solution scattering of biological macromolecules from atomic coordinates. *J Appl Crystallogr* 28:768–773.
27. Baker NA, Sept D, Joseph S, Holst MJ, McCammon JA (2001) Electrostatics of nanosystems: Application to microtubules and the ribosome. *Proc Natl Acad Sci USA* 98:10037–10041.